Design of a Wideband Radio Telescope

W. A. Imbriale,[1] S. Weinreb,[2] and H. Mani[2]

A wideband radio telescope is being designed for use in the Goldstone Apple Valley Radio Telescope program. It uses an existing 34-m antenna retrofitted with a tertiary offset mirror placed at the apex of the main reflector. It can be rotated to use two feeds that cover the 1.2- to 14-GHz band. The feed for 4.0 to 14.0 GHz is a cryogenically cooled, commercially available open-boundary quadridge horn from ETS-Lindgren. Coverage from 1.2 to 4.0 GHz is provided by an uncooled scaled version of the same feed. The performance is greater than 40 percent over most of the band and greater than 55 percent from 6 to 13.5 GHz.

I. Introduction

The Goldstone Apple Valley Radio Telescope (GAVRT) outreach project is a partnership involving NASA, the Jet Propulsion Laboratory (JPL), the Lewis Center for Educational Research (LCER), and the Apple Valley Unified School District, located east of Los Angles near the NASA Goldstone Deep Space Communication Complex. This educational program currently uses a 34-m antenna, DSS 12, at Goldstone for classroom radio astronomy observations via the Internet. The GAVRT program[3] introduces students in elementary, middle, and high school to the process of science with the goal of improving science literacy among American students. The current program utilizes DSS 12 in two narrow frequency bands around S-band (2.3 GHz) and X-band (8.45 GHz) and is heavily subscribed by a training program involving a large number of secondary-school teachers and their classrooms. To expand the program, a joint JPL–LCER project was started in mid-2006 to retrofit an additional existing 34-m beam-waveguide (BWG) antenna, DSS 28, with a wideband feed and receiver to cover the 1.2- to 14-GHz frequency bands.

The antenna to be retrofitted was designed as part of the JPL Antenna Research System Task described in [1]. The antenna, shown in Fig. 1, has a 34-m-diameter main reflector, a 2.54-m subreflector, and a set of beam-waveguide mirrors surrounded by a 2.43-m tube. The antenna was designed for high power and a narrow frequency band around 7.2 GHz. The performance at the low end of the frequency band desired for the educational program would be extremely poor if the beam-waveguide system was used as part of the feed system. Consequently, the revised design uses a wideband feed illuminating a tertiary mirror positioned near the apex of the main reflector. This article will describe the wideband radiometric receiver front end with emphasis on the feed and optical system.
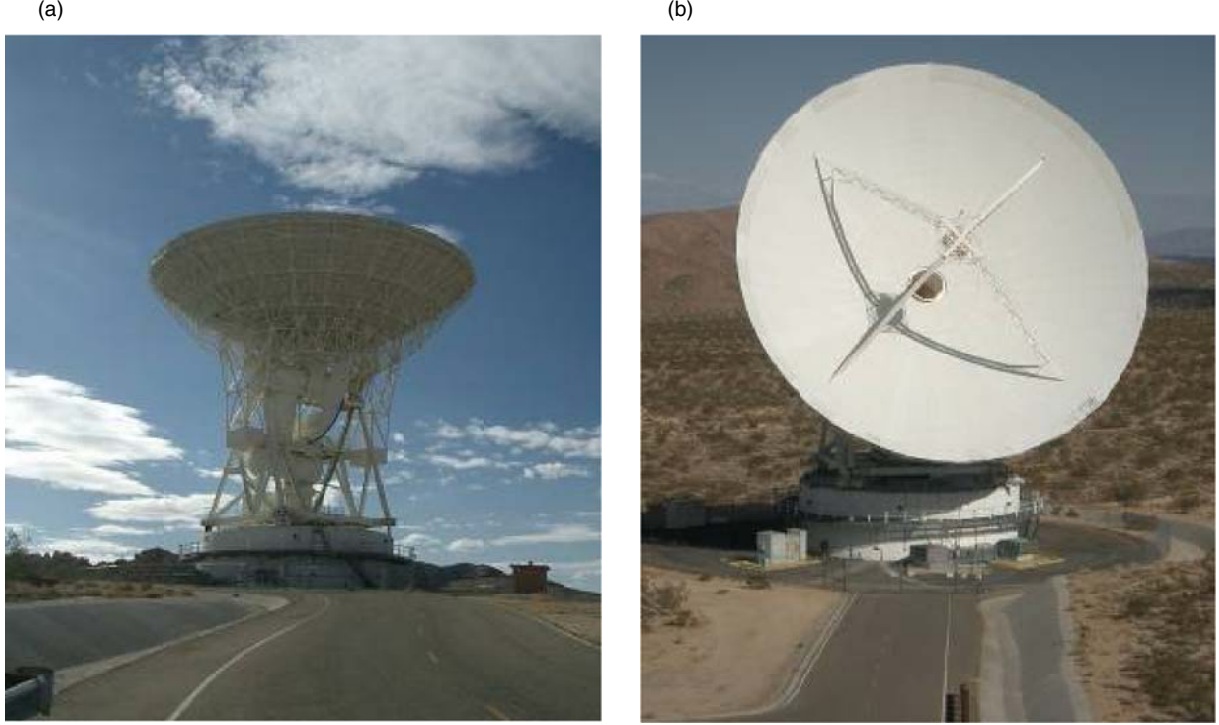
---

[1] Communications Ground Systems Section.

[2] California Institute of Technology, Pasadena, California.

[3] See http://www.lewiscenter.org/gavrt/.

Fig. 1. Photographs of the DSS-27 antenna: (a) side view and (b) front view. It is identical to the DSS-28 antenna, which will be modified for the wideband operation described in this article. The original antenna has a beam-waveguide optical system that guides the beam through the 2.74-m-diameter hole at the vertex, through mirrors, to a large stationary control room in the antenna base. The revised system will utilize a tertiary reflector covering hole with receivers located near the vertex.

II. Radio Astronomy Applications

A key principle of the GAVRT outreach program is the involvement of JPL and other scientists in terms of interest in the data and contact with the teachers through the Lewis Center. This involvement is greatly enhanced by having professional-quality instrumentation that is capable of providing new results of significant scientific value. For this reason, the expansion program will equip DSS 28 with radiometers that have state-of-the-art sensitivity over an unprecedented decade or more of frequency range. The observations that are enabled by the 1.2- to 14-GHz frequency range are

(1) Expansion of the existing DSS-12 S- and X-band observations of the time variation of radio radiation from Jupiter.

(2) Observations of the broadband continuum radio emission from other planets, quasars, supernova remnants, and other astronomical objects where the intensity as a function of frequency gives important information about the physics of the radiation.

(3) Observations of the 1.42-GHz hydrogen line [2]. Hydrogen is the most abundant element in the universe, can be observed in most interstellar regions of our galaxy, and by measurements of the Doppler-shifted line can be used as a probe of radial velocity and radio luminosity of other galaxies. A receiving system capable of 1.2-GHz observations will allow measurements of galaxies with red-shifts up to 0.15 of the velocity of light.

(4) Observations of many radio astronomy molecular lines such as hydroxyl (1.67 GHz), methyladyne (3.3 GHz), formaldehyde (4.8 and 14.5 GHz), methanol (6.7 and 12.2 GHz), helium (8.7 GHz), acetamide (9.2 GHz), and cyclopropenone (9.3 GHz). The strengths and line shapes of these lines allow study of the chemistry in distant region of the universe.

(5) Observations of pulsars—in particular, pulses of sub-nanosecond duration recently discovered by Hankins [3] and requiring wide bandwidth to measure the pulse width. The timing and intensity of many other pulsars are of great interest as probes of gravitational waves and the physics of neutron stars.

(6) Search for signals from extra-terrestrial civilizations.

III. System Design

The complete system involves the reflector, subreflector, tertiary reflector, feed, cryogenics subsystem, low-noise amplifiers (LNAs), noise-calibration system, frequency converters, digital spectrometers, continuum signal processing, and monitor and control system. Only the tertiary, feed, cryogenics, and LNA will be discussed in this article. The main parameters of this front end are the antenna efficiency, η, and the system noise temperature, T_{sys}. Our goal is an η of >40 percent from 1.2 to 14 GHz, with typical values of 55 percent, and a maximum T_{sys} of 55 K over the band, with 35 K at the best frequencies. These values of T_{sys} include 2.7-K cosmic background, 3 K of atmosphere, and 5 K allocated for spillover and feed-support reflections of ground radiation, so 10 K must be added to the noise temperature of the feed and LNA.

We believe that in order to meet the above T_{sys} requirement the wideband feed (which has more loss than narrowband feeds) needs to be cryogenically cooled, at least for frequencies above 3 GHz. A single compact wideband feed covering 1.2 to 14 GHz is under development by Kildal at Chalmers University (see [4]) and may be utilized, but in the next section, we describe a baseline approach with a commercially available feed to cover the 4- to 14-GHz range. In this case, a second feed, which may not be cryogenically cooled, could be scaled in size by 3.5 to cover 1.14 to 4 GHz.

The wideband LNAs required for the system have been under development for many years, and over 100 units of the type shown in Fig. 2 have been assembled, tested at 15 K, and utilized in radio astronomy and physics research systems. When cooled to 15 K, the noise is under 5 K from 1 to 12 GHz when driven from a 50-ohm generator. The computer noise model is available and can be used to determine and optimize the noise for other impedances presented by the feed.

IV. Feed Description and Test Results

Pattern and noise measurements of the ETS-Lindgren Model 3105-64 antenna, designed by V. Rodriguez [5], will be described in this section. Integration of the feed with the cryogenics dewar can have a large effect upon performance. The mechanical configuration is shown in Fig. 3. Other than Teflon in the subminiature version A (SMA) connector, the feed is constructed entirely of aluminum, and no deleterious effects of the cryogenic cooling are expected. (The red polycarbonate rims seen in Fig. 3(b) serve no purpose and were removed for all tests.) Within the outer dewar aluminum cylinder vacuum jacket, there is a 24.1-cm-diameter aluminum radiation shield to prevent thermal coupling of the feed to 300 K. Thermal radiation, of the order of 20 W, enters the window but is mostly blocked by a blanket consisting of 16 layers of 25-μm-thick Teflon film separated by a mesh of fine French wedding veil. Without this blanket it was not possible to cool the feed below 100 K, but with the blanket the temperature measured on the feed was 21 K. Thus, the total thickness of Teflon is 0.4 mm, and with a dielectric constant of 2.1, the total electrical length is $l/38$ at 14 GHz, which will produce negligible reflections. The window material is 1.5-mm-thick high-density polyethylene (HDPE) with a dielectric constant of 2.4. The window electrical length of $l/9.2$ at 14 GHz is not negligible but will not have a large effect upon the measured noise. The total force on the window at 15-psi atmospheric pressure is 518 kg, which produces a perimeter radial stress of 588 psi compared to a 4270-psi yield stress for HDPE. Thus, a better compromise may be a thinner window, but cold flow and creep will also need to be considered.
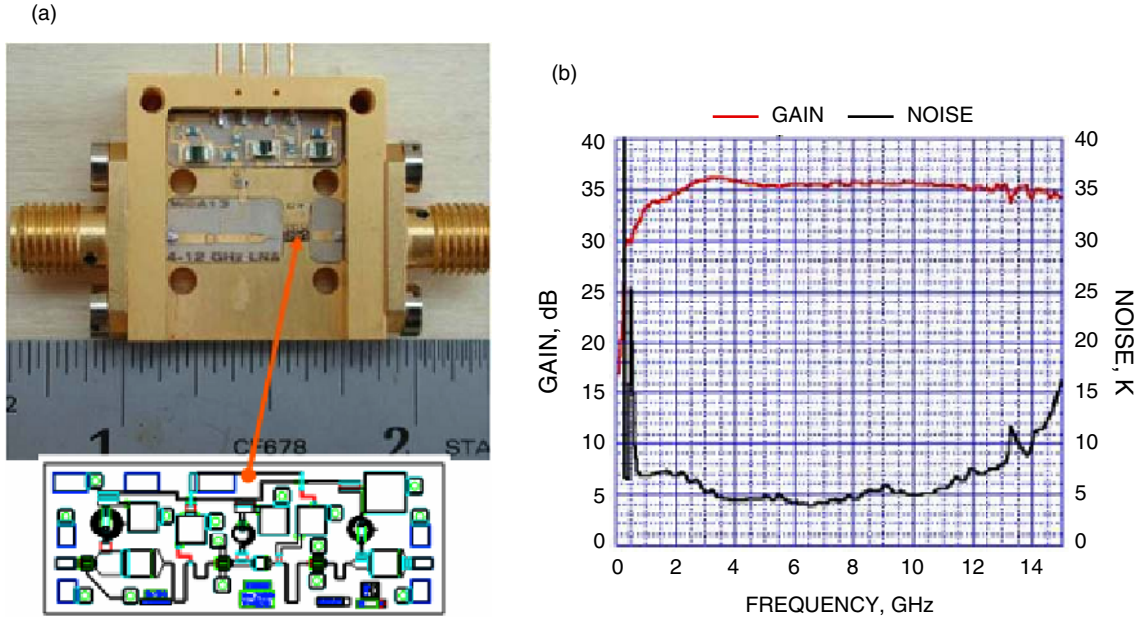
Fig. 2. Cryogenic LNA used in the wideband system: (a) photograph of the three-stage LNA in a 2-mm chip and (b) RF performance.
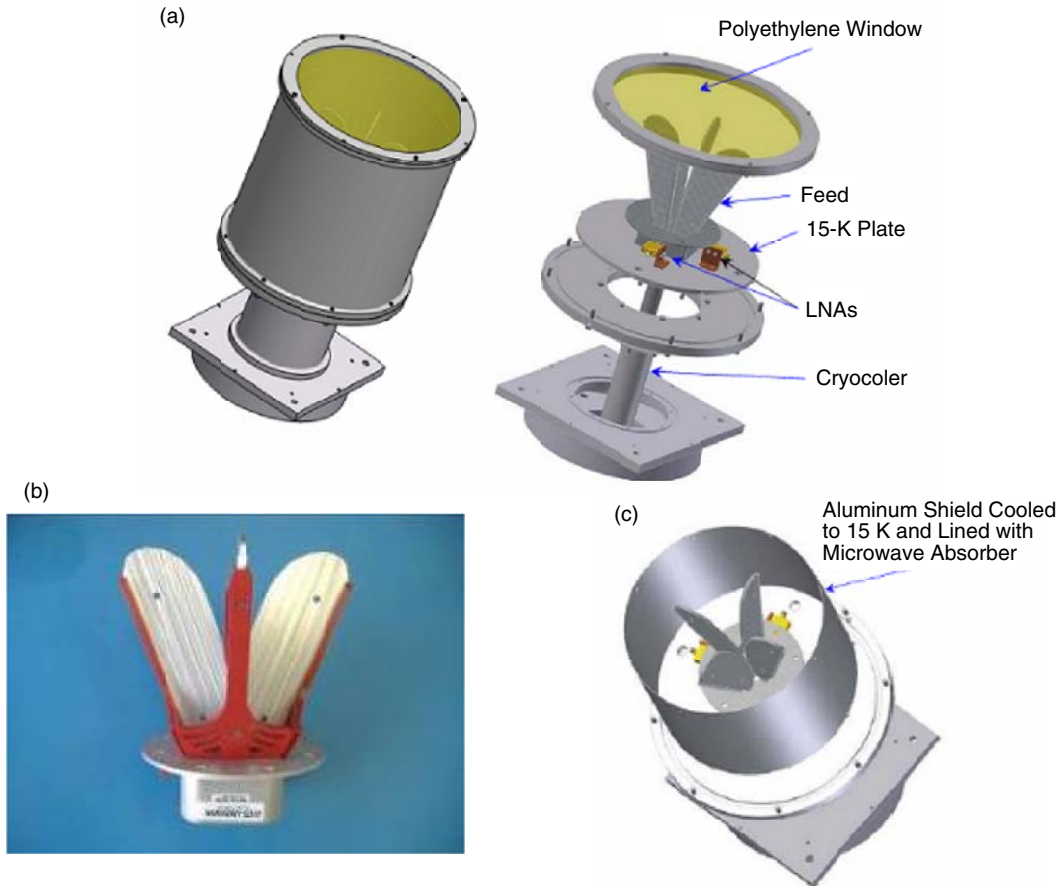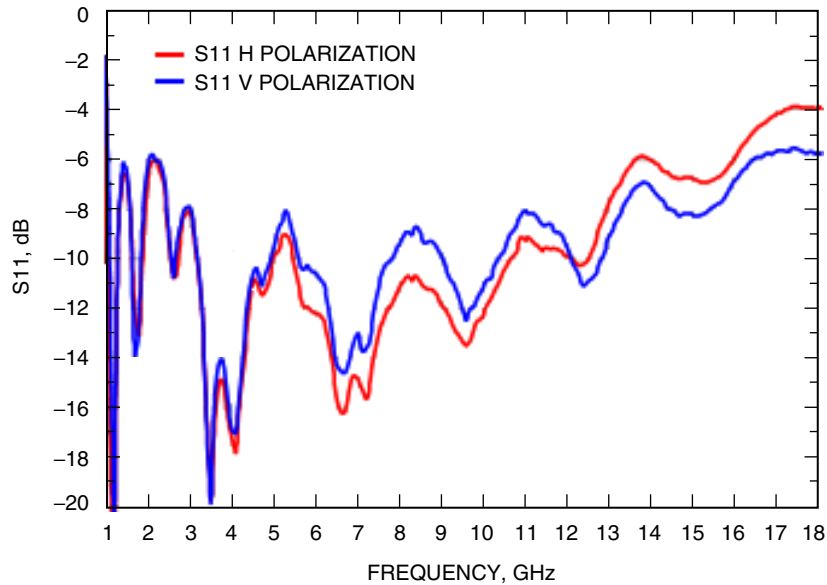

Fig. 3. Integration of the ETS-Lindgren feed in a cryogenic dewar with 30-cm outside diameter: (a) cutaway view showing components (no 15-K shield), (b) ETS-Lindgren feed, and (c) with the 15-K shield.

The feed return loss without a window was measured as shown in Fig. 4. The 2.4-GHz ripple period in the data would arise from two reflections spaced 6.2-cm apart, which is of the order of the spacing of the connector to the radiating region of the slot. The feed has a built-in balun and could be better matched with a differential LNA. Effects of the feed impedance variation are observed in the noise data, and improvements in the noise match to the LNA for particularly important frequencies could be implemented.

The feed patterns were measured with four different configurations of surrounding structures, as shown in Fig. 5, with results compared in Fig. 6. It was found that the pattern for illumination of a reflector could be improved by surrounding the feed with an absorbing cylinder. At a later stage, it was realized that placing absorbing strips of lossy material on the outer surfaces of the fins could have the same effect. Currents flowing around the outer perimeter of the fins thus are absorbed and prevented from coupling to the surrounding cylinder. The question is raised of whether the absorber will deteriorate the efficiency of the feed and add to the noise temperature. Data indicating that the efficiency may not be reduced are shown in Fig. 7, where the transmission loss from the feed to a test antenna in an anechoic chamber is measured. The result shows a decrease in on-axis loss at frequencies below 3 GHz, a small increase in loss from 3 to 6 GHz, and negligible effects above 6 GHz. The noise temperature contributed by the absorber should be small if the absorber is at cryogenic temperatures.
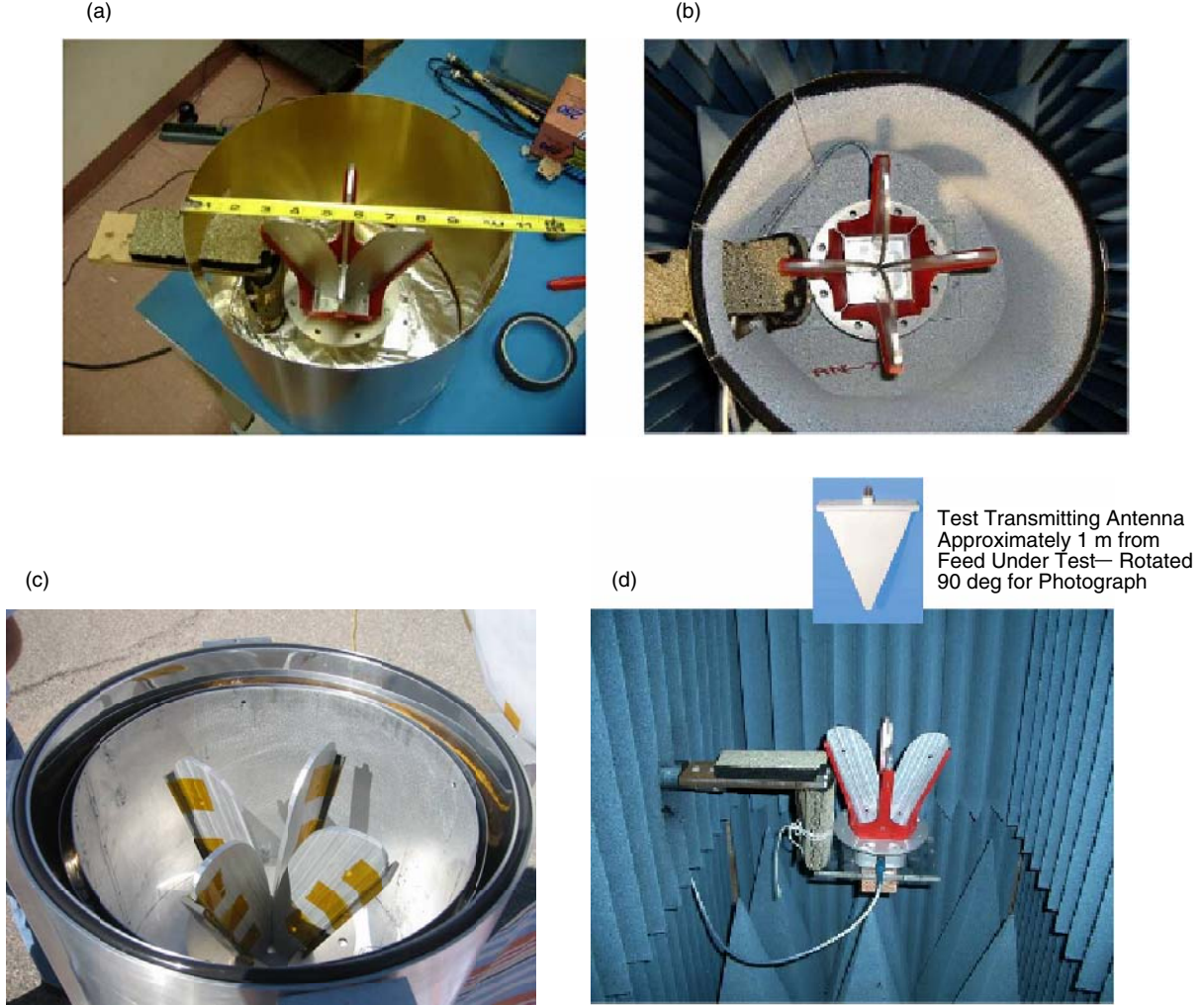
After the pattern tests, the feed was integrated with LNAs on both polarizations and a cryogenics dewar cooled with a closed-cycle CTI Model 350 cryocooler. This cooler has a capacity of 2 W at 14 K and 5.5 W at the measured temperature of 21 K. Cool-down time was approximately 6 hours.

Noise temperature tests of the cooled system were performed both in Pasadena, California, and later in the Mohave desert at Goldstone, California (Fig. 8), to reduce the effects of radio frequency interference (RFI). One polarization had a 4- to 12-GHz LNA with 39-dB gain and <10-K noise from 3 to 14 GHz, increasing to 20-K noise at 2 GHz, while the other polarization had a modified 0.5- to 11-GHz LNA, also with 39-dB gain and <10-K noise from 3 to 14 GHz, but with 15-K noise at 2 GHz. As a check of overloading due to RFI, the total power out of the LNAs was measured with values in the −40 dBm range at Goldstone and −20 dBm in Pasadena. With 39 dB of LNA gain, these values referred to the LNA input are 5 dB and 25 dB above a total receiver noise of 30 K in the 10-GHz bandwidth.

**Fig. 4. Return loss of the two linear ports of the feed. The pattern data are of the H port.**

(a)   (b)

(c)   (d)

Test Transmitting Antenna
Approximately 1 m from
Feed Under Test— Rotated
90 deg for Photograph

Fig. 5. Feed in the dewar and in the pattern test chamber: (a) feed in the aluminum 25-cm-diameter cylinder to simu-
late cryogenics dewar, (b) absorber material inserted in the cylinder for additional tests, (c) with the cylinder, and
(d) without the cylinder.

The LNAs were connected, one at a time, to a room temperature Miteq amplifier with 19 dB of gain driving an Agilent E4407B spectrum analyzer usually set for the 2- to 20-GHz frequency range, 181 points with 3-MHz resolution, but sometimes, as in Fig. 9, to the 1- to 6-GHz frequency range with 1-MHz resolution. The raw data displayed on the spectrum analyzer with the absorber at 289 K and with cold sky, assumed to be 5 K, are shown in Fig. 9. These data then are coupled directly to a laptop computer, where the noise temperature, T, is computed by the Y-factor method, $T = (T_{\text{hot}} - Y * T_{\text{cold}})/(Y - 1)$, where Y is the ratio of hot and cold output noise powers.

The measured noise temperature results are shown in Fig. 10 for data taken in Pasadena, Goldstone, and for the LNA alone. The feed-plus-LNA noise is <35 K from 4.2 to 15 GHz and is 25 K in most of the band. These results are consistent with the T_{sys} goals (on the 34-m telescope, including sky and spillover) of <55 K up to 14 GHz and 35 K at the best frequencies. The results are good but are not understood in view of the <10-K LNA noise. Further tests to investigate and improve the noise temperature are planned. One question is whether the absorbing strips are at the 21-K temperature or are being heated by thermal radiation due to poor contact with the fins.
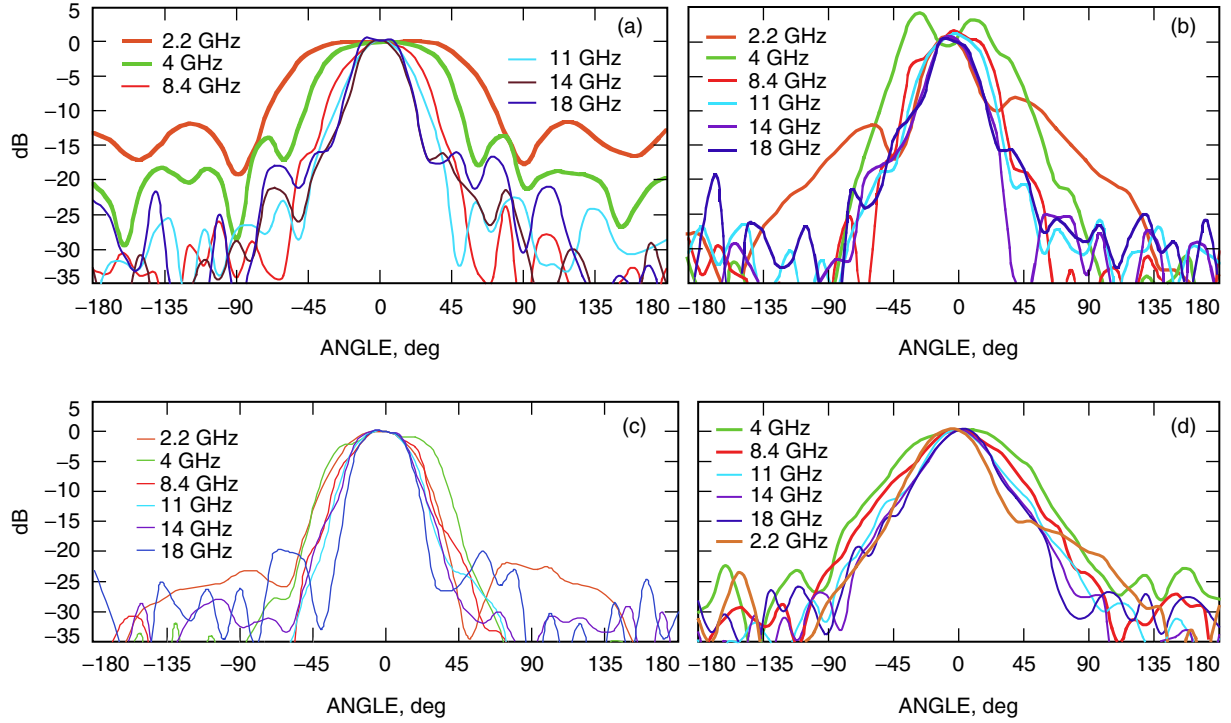
Fig. 6. H-plane patterns of the feed at 6 frequencies and 4 types of enclosures: (a) feed alone, (b) feed in cylinder, (c) feed in cylinder with absorber strips on outside edge of fins, and (d) feed in cylinder with absorber on walls.
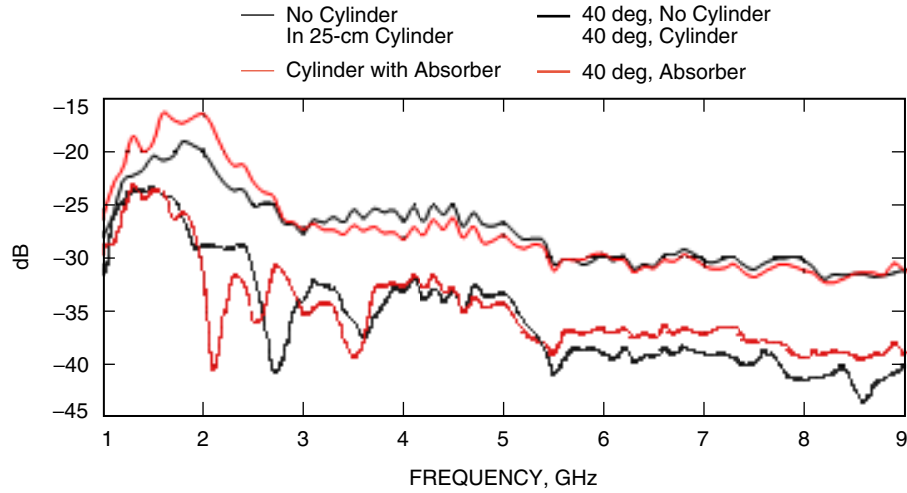
Fig. 7. Transmission in the anechoic chamber from the transmitting antenna to the ETS-Lindgren feed versus frequency with and without the surrounding cylinder lined with the absorber. Curves both on-axis and 40-deg off-axis are shown. Note that below 3 GHz the on-axis transmission is enhanced by approximately 3 dB when the absorber is added.
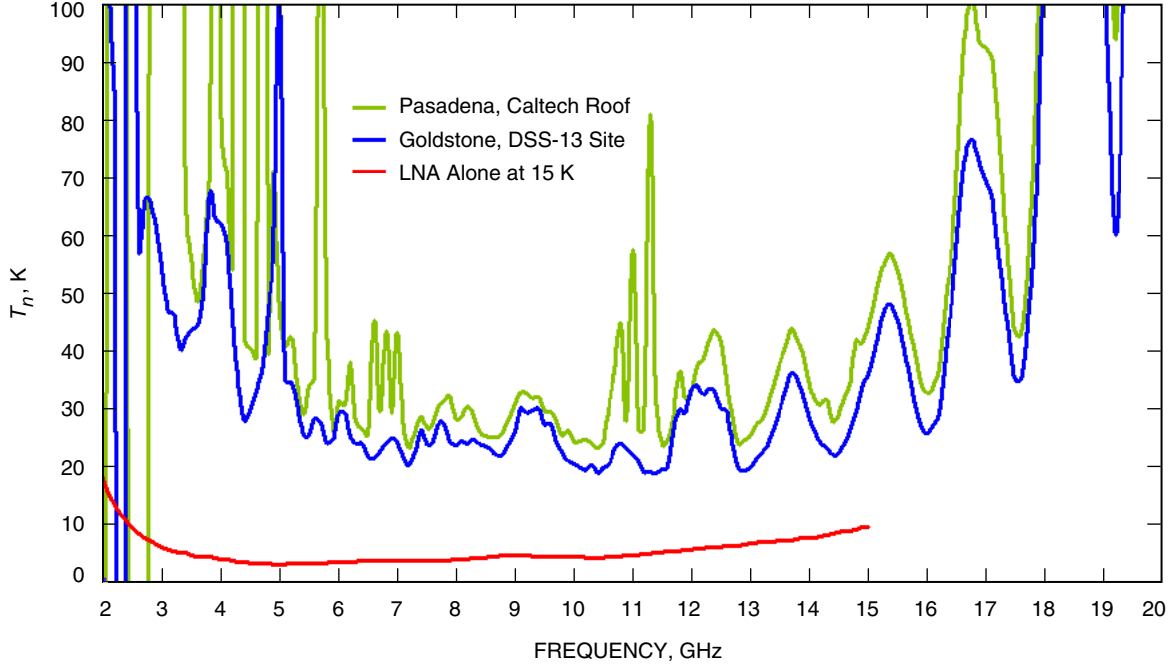
Fig. 8. Test setup for noise measurements of the cooled feed at Goldstone on October 10, 2006, using cold sky and absorber (lower left) on top of the feed window.
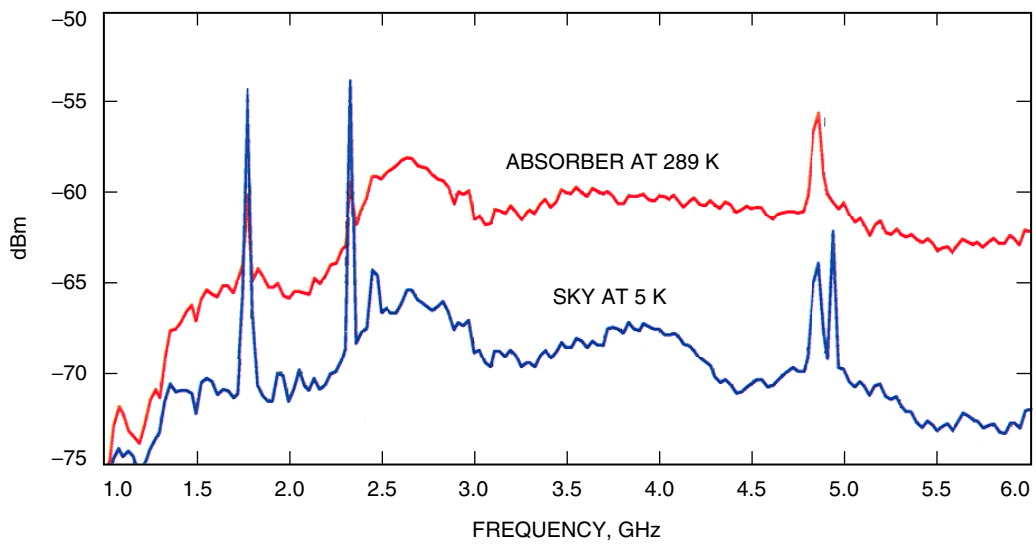
Fig. 9. Raw data spectrum analyzer plots of LNA output power with absorber covering the feed and with the feed viewing cold sky. A ratio, Y-factor, of 9 dB gives a noise temperature of 36 K. The spikes are due to RFI.

8

Fig. 10. Noise temperatures of the feed and LNA as a function of frequency for measurements in Pasadena and Goldstone, and of the LNA alone measured at 15 K, referred to its coaxial input jack. The noise is under 35 K from 4.3 to 15 GHz.

V. Optics Design Trade-Offs

The antenna to be retrofitted is a 34-m beam-waveguide antenna designed as part of the JPL Antenna Research System Task described in [1]. The original antenna geometry is shown in Fig. 11. In contrast to a typical beam-waveguide antenna that traditionally has two curved mirrors to image a feed at the input focal point of a dual-reflector antenna, for this original design only one curved mirror—a paraboloid—is used, along with three flat mirrors. The radiation from the feed horn is allowed to spread to the paraboloid, where it is focused to a point at infinity. That is, after reflection, a collimated beam exists that is directed to the subreflector by the three flat reflectors. The energy is contained in the 2.743-m diameter of the BWG tube and does not begin to spread significantly until it exits through the main reflector. Since a collimated beam exists beyond the first mirror, this antenna is closely related to a near-field Cassegrain design, where the feed system is defined to include both the feed horn and a parabolic mirror.

In a near-field Cassegrain design, both the main reflector and the subreflector are nominally paraboloids, with dual-reflector shaping used to increase the illumination efficiency on the main reflector by compensating for the amplitude taper of the feed radiation pattern. The design of the dual-shaped antenna is based upon geometrical optics, with the shape of the subreflector chosen to provide for uniform amplitude illumination of the main reflector, given the distribution of the radiation striking the subreflector. The curvature of the main reflector is then modified slightly from that of the parent paraboloid to compensate for any phase errors introduced by the subreflector shaping.

The antenna was designed for high power and a narrow frequency band around 7.2 GHz. The performance at the low end of the frequency band desired for the educational program would be extremely poor if the beam-waveguide system were used as part of the feed system. Hence, several redesign options to enable improved performance on the low frequency without the use of the beam-waveguide itself were
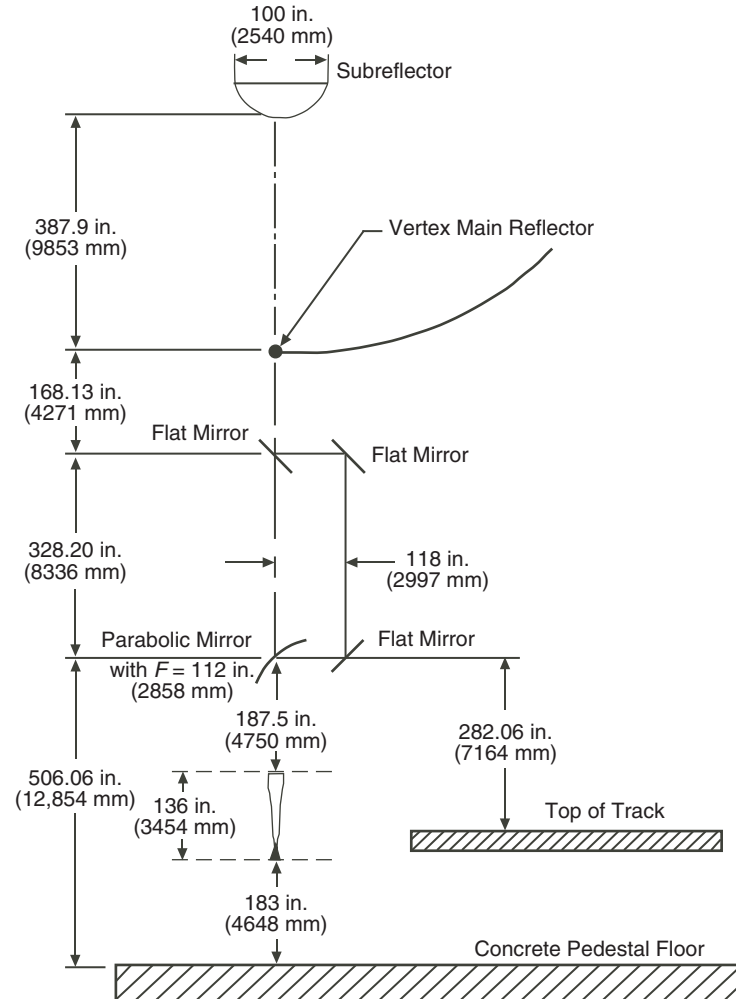
Fig. 11. Geometry of the DSS-28 antenna.

examined. They included (1) redesigning the subreflector and using the broadband feed in a dual-reflector system, (2) using a symmetric 2.54-m reflector tertiary reflector placed at the dish vertex, (3) using a 90-deg 2.54-m offset-design tertiary reflector at the dish vertex, (4) replacing the upper flat mirror with a parabola and placing the feed in the upper portion of the beam-waveguide tube, and (5) using a 60-deg 2.3-m tertiary mirror at the dish vertex. Relative performance was computed using an idealized feed pattern that approximated the type of feed to be used.

From a purely efficiency standpoint, the feed placed at the focal point of a shaped dual-reflector antenna was best. However, since the optics design of the existing system did not have a usable focal point, the subreflector would have to be replaced with one with an appropriate design and the main reflector panels reset for the new subreflector design. Also, since the feed has a very broad pattern, the feed would need to be placed near the subreflector, necessitating the use of a tall feed tower to support it or the hanging of the feed from the subreflector. Also, it would be difficult to access the feed system for maintenance and replacement. For both cost and logistical reasons, this option was rejected.

The next best performing option was a symmetric parabola placed at the vertex of the dish. Since the feed blockage would be small, the only other disadvantage of this option was that it would not be able to easily switch between feeds if, to cover the frequency band, more than one feed were required. The

offset options allowed the use of a rotating reflector that would be able to easily switch between multiple feeds. Since this is to be an educational tool, flexibility and versatility are extremely important. Hence, this option was rejected.

For the offset options, the parabola at the flat mirror position performed poorly at the lowest frequencies. The performances for the other two offset options were virtually identical, so the design with the smaller parabola was selected.

VI. Optics Design Optimization and Performance

Amplitude and phase co-polar and cross-polar patterns of the Lindgren feed were measured at fin angles of 0, 45, 90, and 135 deg and for feed rotation angles of -180 to $+180$ deg in 10-deg steps. The data were taken for the feed with absorber strips on the fin outer surfaces and a metal cylinder surrounding the feed. These data were then used to optimize the design of the tertiary reflector. Frequencies of 4 and 12 GHz were selected for optimization. The parameters to be optimized were focal length, diameter, offset height, feed tilt angle, and feed defocusing. An optimization program was used, and the parameters were determined that yielded the highest peak gain. Using the geometry shown in Fig. 12, the optimum parameters for 4 GHz are $F = 1.38$ m, $D = 2.24$ m, $\theta_f = 47$ deg, $h = 7.7$ cm, and $\Delta Z = -0.32$ cm. The optimum parameters for 12 GHz are $F = 1.27$ m, $D = 2.25$ m, $\theta_f = 49.3$ deg, $h = 8.7$ cm, and $\Delta Z = 1.12$ cm. Data for the Lindgren feed were take every 50 MHz from 4 to 14 GHz, and the calculated performances for the two designs are shown in Fig. 13. The layout in the DSS-28 reflector is pictured in Fig. 14. A scaled design feed is going to be used for the 1.2- to 4-GHz band, and the parabola will be rotated to point to the second feed position. The performance for this lower frequency band and the scaled feed is shown in Fig. 15.

VII. Conclusion

The design of a wideband radio telescope to be used as part of the GAVRT educational program has been described. It makes use of an existing 34-m antenna that will be retrofitted with a tertiary offset mirror placed at the apex of the main reflector. It can be rotated to use two feeds that cover the 1.2- to 14-GHz band. The feed for 4.0 to 14.0 GHz is a cryogenically cooled commercially available feed from ETS-Lindgren. Coverage from 1.2 to 4.0 GHz is provided by an uncooled scaled version of the same feed. The performance is greater than 40 percent over most of the band and greater than 55 percent from 6 to 13.5 GHz.
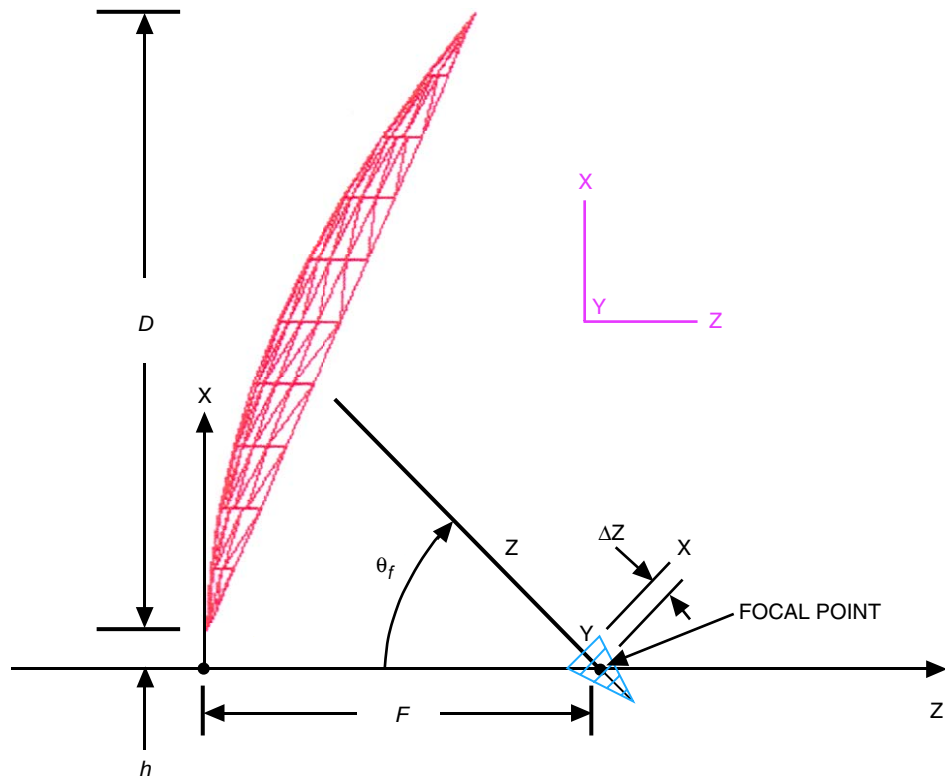
Acknowledgment

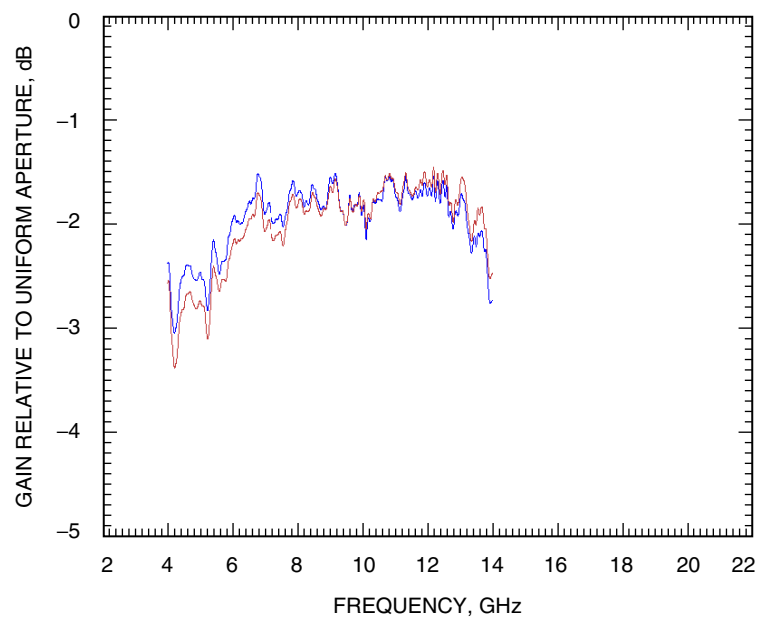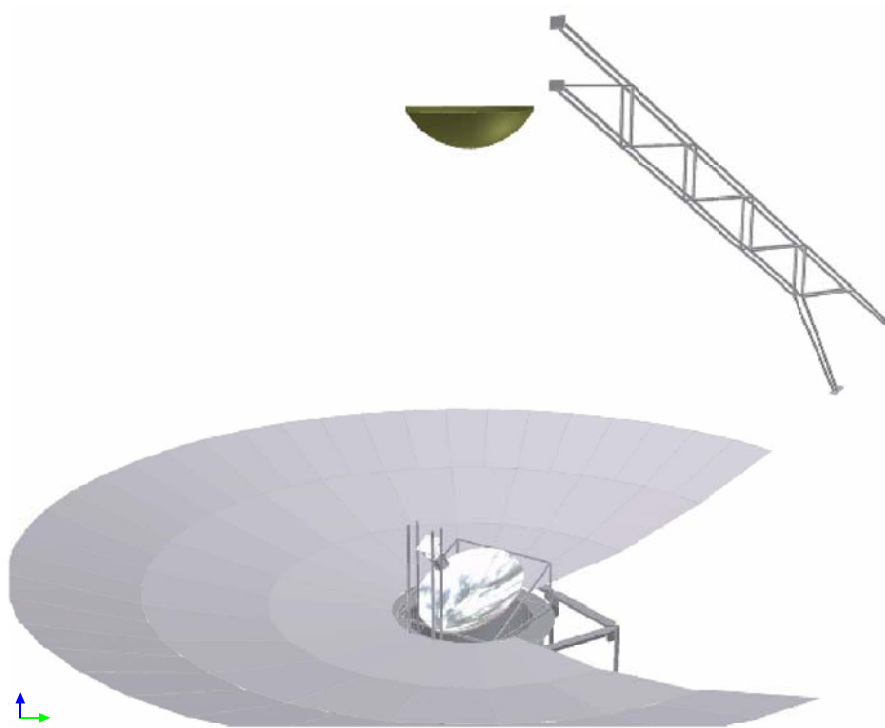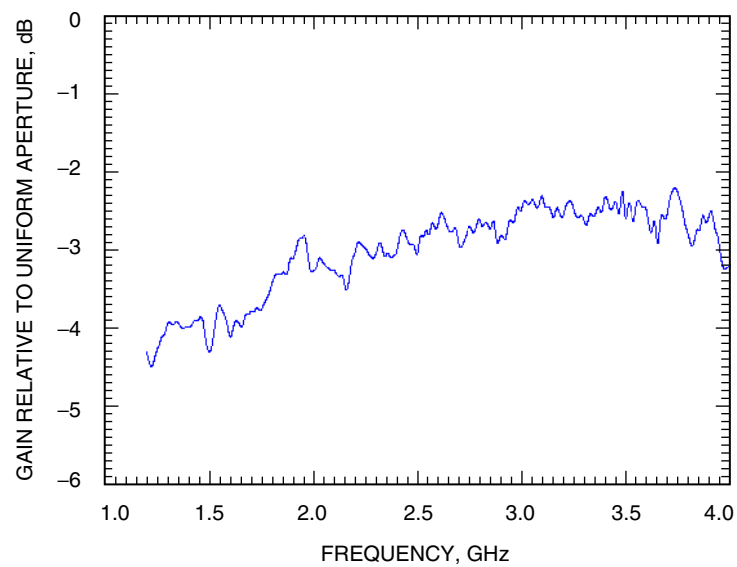**Fig. 12. Geometry of the tertiary reflector.**

Fig. 13. Calculated peak gain performance of the cryogenically cooled Lindgren feed. Comparison of the tertiary reflector optimized for 4 GHz (blue) and 12 GHz (red).

Fig. 14. Layout of the tertiary mirror in the main reflector.

**Fig. 15. Performance of the scaled uncooled
lower-frequency feed.**

References

[1] W. A. Imbriale, *Large Antennas of the Deep Space Network*, Chapter 9, Hoboken, New Jersey: Wiley Interscience, 2003.

[2] B. B. Burke and F. Graham-Smith, *An Introduction to Radio Astronomy 2nd Edition*, Cambridge, United Kingdom: Cambridge Press, pp. 154–159, 2002.

[3] T. Hankins, "Nanosecond Bursts from Strong Plasma Turbulence in the Crab Pulsar," *Nature*, vol. 422, pp. 141–143, March 13, 2003.

[4] R. Olson, P. S. Kildal, and S. Weinreb, "The Eleven Antenna: A Compact Low-Profile Decade Bandwidth Dual Polarized Feed for Reflector Antennas," *IEEE Transactions on Ant. and Prop.*, vol. 54, no. 2, part 1, pp. 368–375, February 2006.

[5] V. Rodriguez, "A Multi-Octave Open-Boundary Quad-Ridge Horn Antenna for use in the S to Ku-bands," *Microwave Journal*, vol. 49, no. 3, pp. 84–92, March 2006.